

Pioneer Venus Orbiter Electron Temperature Probe

J.P. Krehbiel, L.H. Brace, R.F. Theis, J.R. Cutler, W.H. Pinkus, and R.B. Kaplan

ABSTRACT - The Orbiter Electron Temperature Probe (OETP) instrumentation and measurement technique has been designed to perform in-situ measurements of electron temperature and electron and ion density in the ionosphere of Venus. Adaptive sweep voltage circuitry continuously tracks the changing electron temperature and spacecraft potential while auto-ranging electrometers adjust their gain in response to the changing plasma density. Control signals used in the instrument to achieve this automatic tracking provide a continuous monitor of the ionospheric parameters without telemetering each volt-ampere curve. Internal data storage permits high data rate sampling of selected raw characteristic curves for low rate transmission to Earth. These curves are used to verify or correct the inflight processed data. Sample in orbit measurements are presented to demonstrate instrument performance.

I. INTRODUCTION

THE PIONEER VENUS Orbiter Electron Temperature Probe (OETP) is one of several instruments used on the orbiter to perform *in-situ* measurements of the ionospheric plasma of Venus. The instrument employs cylindrical Langmuir probes to measure the electron temperature, T_e , the electron and ion densities, N_e and N_i , and the spacecraft potential, V_s . To provide high spatial resolution of these parameters the instrument takes several hundred volt-ampere curves during each brief passage through the ionosphere. Owing to the limited telemetry rate available to each instrument, circuitry was included for inflight processing of the volt-ampere curves. Onboard storage of raw data from selected curves was provided to permit ground confirmation of the inflight processing method. Prior to launch, the instrument design was outlined briefly by Brace in a paper edited by Colin and Hunten (1977) [1]. The purpose of this paper is to present a more detailed account of the instrument and some of the data acquired at Venus to illustrate how the instrument performs and how the ground data analysis is used to verify the flight measurements. Early results from this experiment have been reported [2] - [4].

II. THEORY OF THE METHOD

The OETP is the latest spaceflight version of cylindrical electrostatic probe of Langmuir probe instrumentation. I. Langmuir and H. Mott-Smith, Jr., first reported use of the electrostatic probe in a laboratory plasma in 1924 [5]. The cylindrical probe technique has been used extensively to characterize the Earth's ionosphere [6], most recently on board the Atmosphere Explorer (AE) satellites [7]. The three AE instruments with their adaptive control circuitry and auto ranging electrometer provided the basis for the OETP instrument.

Langmuir probe theory and application has been widely reported in the literature [1] - [8]. Here it will suffice to provide a brief description of the technique and to remind the reader of the theoretical volt-ampere curve produced by a Langmuir probe in a plasma as shown in Fig. 1. The curve begins in the ion saturation region with the probe potential sufficiently negative to prohibit plasma electrons from reaching the probe. At this point, current to the probe is due only to ions. In the retardation region where the probe potential is less negative, the more energetic electrons overcome the retarding potential, and produce an exponentially increasing current. The electron temperature T_e determines the power of the exponential with lower T_e yielding a narrower retarding region. In the electron saturation region, the probe is positive with respect to the plasma and therefore attracts additional electrons from the plasma. Equations appropriate to the three regions of the curve are given below.

In the ion saturation region at 90° angle of attack [8]

$$I_i = AN_i e w / \pi (1 + k T_i / m_i w^2 + 2eV / m_i w^2)^{1/2} \quad (1)$$

In the electron retardation region [2]

$$I_e = AN_e e (k T_e / 2 \pi m_e)^{1/2} \exp(eV / k T_e). \quad (2)$$

In the electron saturation region [9], [10]

$$I_e = (AN_e e / \pi) (2eV / m_e)^{1/2} \quad (3)$$

where

N_e	electron density
N_i	ion density
T_e	electron temperature
T_i	ion temperature
A	collector surface area
w	collector speed with respect to plasma
k	Boltzmann constant
m_i	mean ion mass
m_e	electron mass
V	collector voltage with respect to the plasma
e	electron charge.

OETP measurements are made with respect to spacecraft ground. This causes the voltage applied to the probe V_A to be translated by the spacecraft potential V_s , as illustrated in [Fig. 1](#). Special steps must be taken to account for this and to assure a stable spacecraft potential. This will be described later.

III. THE EXPERIMENTAL ARRANGEMENT

The OETP instrumentation system consists of two cylindrical sensors and a central electronics unit. [Fig. 2](#) illustrates the relative position of the sensors and the larger appendages of the spacecraft. The radial sensor is mounted at the end of a 1-m boom which was folded against the solar array and deployed after Venus orbit insertion so as to be perpendicular to the spacecraft spin axis. The axial sensor is mounted on a fixed boom which places it 0.4 m away from the spacecraft forward surface. Because the axis of the axial sensor is parallel to the spin axis it maintains a relatively constant angle of attack to the incident plasma and is therefore not subject to spin modulation.

To provide an adequate path for return current to the plasma, the spacecraft provides 1.73 m² of exposed conducting area which is spacecraft ground. This area consists of a metal band around the solar array, a metal mesh over the outer kapton surface of the forward thermal blanket, and the outer surface of the magnetometer boom. Silicone rubber was applied to all solar cell edges and exposed electrical conductors making up the solar array to insulate these positive potential areas from the plasma and thus minimize the electron current they would otherwise collect producing a concomitant change in spacecraft potential.

A. The Central Electronics

The OETP central electronics unit contains independent electrometer amplifiers and adaptive sweep voltage circuitry to service each probe. [Fig. 3](#) is a simplified functional block diagram of the system. Each amplifier feeds its output into the common A/D converter and data handling circuitry. The autoranging electrometer and adaptive sweep voltage circuits are identical to that employed in the three AE missions [\[7\]](#). The signal multiplexing (Mux), A/D conversion, data formatting, and First-In/First-Out memory (FIFO) are new features to permit the inflight processing and recovery of data, a capability required by the lower data rate available from the orbiter. The radial probe electrometer has a sensitivity range of 1×10^{-10} to 1×10^{-6} A/V, while the axial probe electrometer has a sensitivity range of 1×10^{-9} to 1×10^{-5} A/V. Electrometer sensitivity is automatically adjusted to one of 1024 possible values. Electrical power is provided by a common dc/dc converter having separate floating outputs for each of the two electrometers.

Adaptive circuitry is provided to adjust the sweep voltage to resolve that region of the volt-ampere curve needed to derive N_i , N_e , T_e , and V_s and to track changes in T_e and V_s encountered along the orbit. The adaptive process provides a more continuous monitor of these plasma parameters than could be obtained if we were to rely solely on ground-based analysis of volt-ampere curves produced by the instrument, given the available data rate. The V_A generator converges on the proper starting value V_A Start, and the proper rate of change V_A Slope through an iterative process involving the auto-ranging electrometer and the adaptive V_A circuitry. When the adaptive process is completed, usually within two sweeps, the curves are properly framed to maximize the resolution of the measured parameters. Once proper framing had been achieved, it is maintained by slight adjustments in V_A Start, V_A Slope, and electrometer gain which track the changes in electron temperature, density, and spacecraft potential.

An idealized $\frac{1}{2}$ -s instrument measurement cycle of applied voltage, and the resulting electrometer output for a properly framed curve are shown in [Fig. 4](#). Also shown are the parameters used to carry out the adaptive process and to achieve the inflight analysis. The cycle begins at time T_0 by setting V_A equal to V_A Start as determined from parameters measured during the previous curve. After a settling time the electrometer auto-ranging algorithm is initiated to adjust the electrometer gain as needed to drive its output to the -3.30-V threshold. Current to the sensor at this time is entirely ion current and is used to determine N_i . At time T_1 the V_A is increased linearly at a rate also determined from the previous curve. The V_A and electrometer outputs are monitored by level detectors. When the electrometer output reaches +1.41 V a level detector starts a counter and the value of V_A at T_2 is measured. When the electrometer

output reaches +9.50 V, a second level detector stops the counter and the value of V_A at T_3 is measured. At T_3 the electrometer downranges by one decade and displays the rest of the volt-ampere curve until the linear sweep is stopped at T_4 . At T_4 a fixed 2-V step is added to drive the sensor into the electron saturation region. The electrometer then downranges until its output is on scale and a reading of output voltage and gain are taken and used to determine N_e .

In each 1/2-s instrument cycle we are thus able to determine, from each electrometer, N_i from the gain and electrometer output just prior to T_1 , T_e from the change in V_A which produced a factor of e change in electrometer output, and N_e from the gain and electrometer output during the N_e sample time. The curve framing process continues by automatically computing new values of V_A Slope and V_A Start. V_A Slope is computed from our definition of a properly framed curve which requires that the full amplitude of V_A be ten times the value of the change in V_A from T_2 to T_3 when the 1.41- and 9.50-V thresholds are reached. V_A Start is computed using (4) which places the exponential electron retardation region such that the 9.50-V threshold is reached at 86 percent of the sweep interval.

$$V_A \text{ Start} = 8.6 V_A \text{ at } T_2 - 7.6 V_A \text{ at } T_3. \quad (4)$$

If the V_A at T_1 does not provide a net ion current to the collector or if the electrometer fails to reach the +9.50-V output, called the T_3 threshold, the VA generator will preset to the "fault" condition for the next sweep causing V_A to start at -7 V and sweep up to +5V. The fault sweep amplitude is sufficient to locate the operating region of the volt-ampere curve and to permit the convergence algorithm to repeat at the beginning of the following sweep.

As a safeguard against unforeseen difficulties which might cause our adaptive approach to fail, a fixed amplitude sweep mode can be selected by ground command in which a sequence of high and low voltage sweeps are applied to either or both sensors. The high V_A was -7 to +5 V and the low V_A was -2 to +1 V. In this mode a bias voltage of +/- 1 V can be added to account for V_s uncertainties. The fixed sweep mode is not normally used because the adaptive mode yields better resolved stored curves.

B. The Sensors and Booms

A sensor with its guard electrode and a portion of the boom are schematically shown in [Fig. 5](#). The guard electrode, driven at V_A , is the exposed inner shield of a rigid triaxial boom fabricated with titanium and teflon. The outer triaxial shield is held at spacecraft ground potential. A special white conductive paint, GSFC Code No. NS43C [\[11\]](#), was applied to the outer surface of the booms to provide thermal control. Flight sensors were screwed onto the boom center conductor and held in place with a high temperature silicone (Dow Corning X 12561, silver filled for electrical conductivity) to assure that the sensors remained in place during the launch vibration.

The accuracy of the temperature measurements is affected by the characteristics of the sensor surface [\[12\]](#). In particular, the work function of different crystal surfaces can vary by as much as several tenths of a volt and thus introduce an uncertainty in the value of V in [\(1\)-\(3\)](#). To reduce this error the collectors were fabricated using a chemical vapor deposition CVD process. Studies of the CVD Rhenium show that Rhenium deposited by the pyrolytic decomposition of Rhenium pentachloride (ReCl_5) show a very high degree of crystal orientation. Rhenium deposited in this manner exhibits a (0001) preferred orientation [\[13\]](#) perpendicular to the plane of growth. Cylindrical tubes of this type have yielded uniform vacuum work functions of 5.1 eV. Molybdenum deposited from MoCl_6 also shows a very high degree of crystal orientation. Thus both materials become candidates for sensor materials.

[Fig. 6](#) shows part of a cross section of a collector having a CVD Rhenium surface deposited on a polycrystalline substrate. Flight collectors were selected on the basis of examining similar cross sections cut from one end of the collector and from volt-ampere curves taken in laboratory plasmas. The radial collector surface is Rhenium and the axial is Molybdenum.

C. Measurements Format

The orbiter is able to operate in several data formats and at spacecraft data rates from 16 to 2048 b/s. The OETP is designed for optimum operation when its output data rates are 80, 128, or 160 b/s, one of which is normally used during a periapsis pass. Various instrument data formats can be selected by command to provide for more or less dense coverage depending on such factors as spacecraft bit rate and whether the OETP data system is dedicated to one sensor or shared by both of them.

IV. VERIFICATION OF INFLIGHT ANALYSIS

To permit ground calibration of the values of Ni, Ne, and Te determined by the inflight processing, the instrument periodically samples volt-ampere curves from either or both electrometers. The electrometer output is measured at 50 equally spaced points between T_1 and T_4 . The FIFO memory is used to store the fifty measurements, made at 1132 b/s, for later readout at the lower spacecraft telemetry rate. [Fig. 7](#) illustrates the ground analysis of such a stored curve taken from orbit 112. The solid line represents a least squares fit of a straight line (ion current) and exponential (electron current) to the actual data points within the electron retardation region.

V. ILLUSTRATION OF OPERATION AT VENUS

Fig. 8 is a computer plot of the values of T_e and N_e taken from a single pass of the orbiter through the nightside ionosphere. The line segments connect the inflight values and reveal the small-scale spatial structure which is often present. The asterisks represent the values of T_e and N_e derived later by computer fitting stored volt-ampere curves of the type illustrated in Fig. 7. Values derived from the stored curves are used to normalize the inflight processed data. Thus through the use of on-board processing of curves, high spatial resolution is achieved without sacrificing the accuracy provided by ground computer fitting of raw volt-ampere curves. As of this writing more than 250 passes through the ionosphere of Venus have been completed and the instrument continues to operate well.

ACKNOWLEDGEMENT

The authors gratefully acknowledge the aid of L.R.O. Storey in the testing of candidate collectors in the low temperature plasma chamber at the Centre de Recherches en Physique de L'Environnement Terrestre et Planetaire in Orleans, France.

REFERENCES

- [1] L.H. Brace, "Orbiter electron temperature Probe," L. Colin and D.M. Hunten, Eds. Space Sci. Rev., vol. 20, no. 4, P.454, June 1977.
- [2] L.H. Brace, R.F. Theis, J.P. Krehbiel, A.F. Nagy, T.M. Donahue, M.E. McElroy, and A. Pedersen, "Electron temperatures and densities in the Venus ionosphere," Science, vol. 203, p. 763, Feb. 23, 1979.
- [3] L.H. Brace, H.A. Taylor Jr., P.A. Cloutier, R.E. Daniell Jr., and A.F. Nagy, "On the configuration of the nightside Venus ionopause," Geophys. Res. Lett., vol. 6, p. 345, 1979.
- [4] L.H. Brace, R.F. Theis, H.B. Niemann, H.G. Mayr, W.R. Hoegy, and A.F. Nagy, "Empirical models of the electron temperature and density in the nightside Venus ionosphere," Science, vol. 205, p. 102, 1979.
- [5] I. Langmuir, and H. Mott-Smith, Jr., "Studies of the electric discharges in gases at low pressures," Gen. Elec. Rev., p. 616, Sept. 1924.
- [6] L.H. Brace, "Global structure of ionosphere temperature," in Space Research X. Amsterdam, The Netherlands: North-Holland, p. 633, 1970.
- [7] L.H. Brace, R.F. Theis, and A. Dalgarno, "The cylindrical electrostatic probes for atmosphere explorer -C, -D, -E," Science, vol. 8, no. 4, p. 341, Apr. 1973.
- [8] W.R. Hoegy and L.E. Wharton, "Current to moving spherical and cylindrical electrostatic probes," J. Appl. Phys., vol. 44, no. 12, p. 5365-5371, 1973.
- [9] H. Mott-Smith and I. Langmuir, "The theory of collectors in gaseous discharges," Phys. Rev., vol. 28, pp. 727-763, 1926.
- [10] N.W. Spencer, L.H. Brace, G.R. Carignan, D.R. Taesch, and H.B. Niemann, "Electron and molecular nitrogen temperature and density in the thermosphere," J. Geophys. Res., vol. 70, pp. 2665-2698, 1965.
- [11] M.C. Shai, "Formulation of electrically conductive thermal-control coatings," NASA Tech. Paper 1218, Apr. 1978.
- [12] D. Smith, "The application of Langmuir probes to the measurement of very low electron temperatures," Planet. Space Sci., vol. 20, p. 1721, 1972.
- [13] L. Yang, "Preparation & evaluation of CVD rhenium thermionic emitters," in The Third Annual Conference on Chemical Vapor Deposition, F.A. Glaski, Ed., American Nuclear Society, 1972.

Fig. 1. A theoretical volt-ampere characteristic of a cylindrical collector in a plasma showing the three regions of the curve from which N_i , T_e , N_e , and V_s may be derived. Note: The current scale in the ion saturation region is enlarged for illustrative purposes.

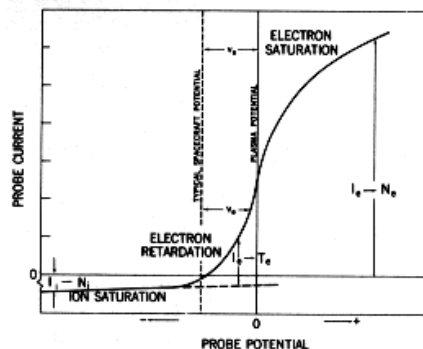


Fig. 2. Langmuir probe mounting locations on the PV orbiter spacecraft. The axial sensor generally looks forward along the orbit path when the spacecraft is passing through the ionosphere. 1.73 m² of bare metal area on the spacecraft is exposed to the plasma to provide a return path for the current to the sensors. The sensors and their exposed guard electrodes make up the last 7.5 cm of their respective booms.

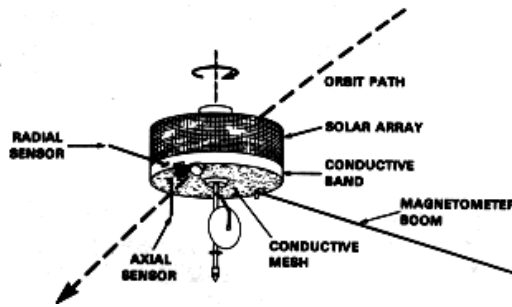


Fig. 3. A simplified block diagram of the OETP showing the elements necessary to operate one sensor.

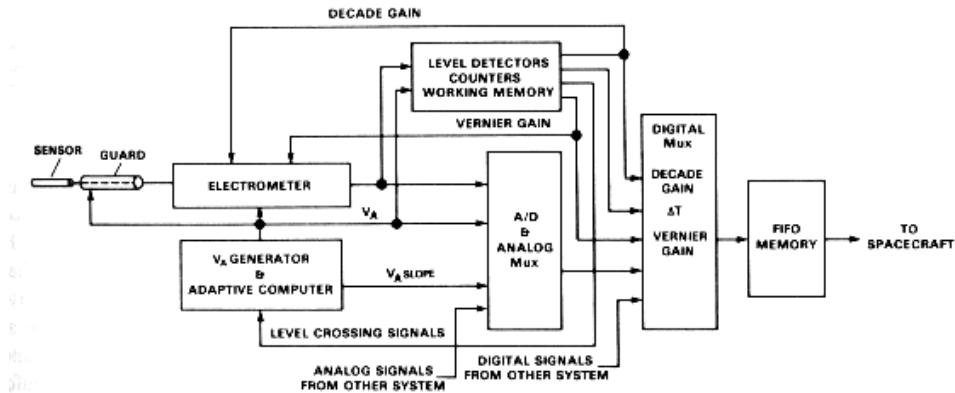


Fig. 4. An idealized single volt-ampere curve illustrating the various functions occurring within each instrument cycle.

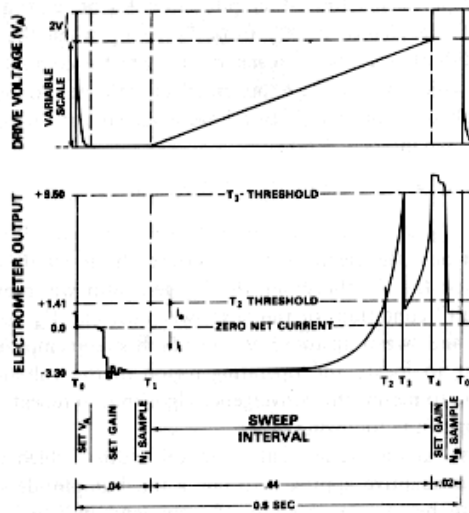


Fig. 5. A detailed view of the sensor.

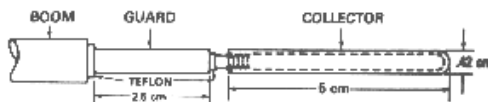


Fig. 6. A photomicrograph of a cross section of a Rhenium sensor. The aligned crystals were grown on the polycrystalline substrate using a chemical vapor deposition process resulting in a sensor surface having a uniform work function of 5.1 eV.

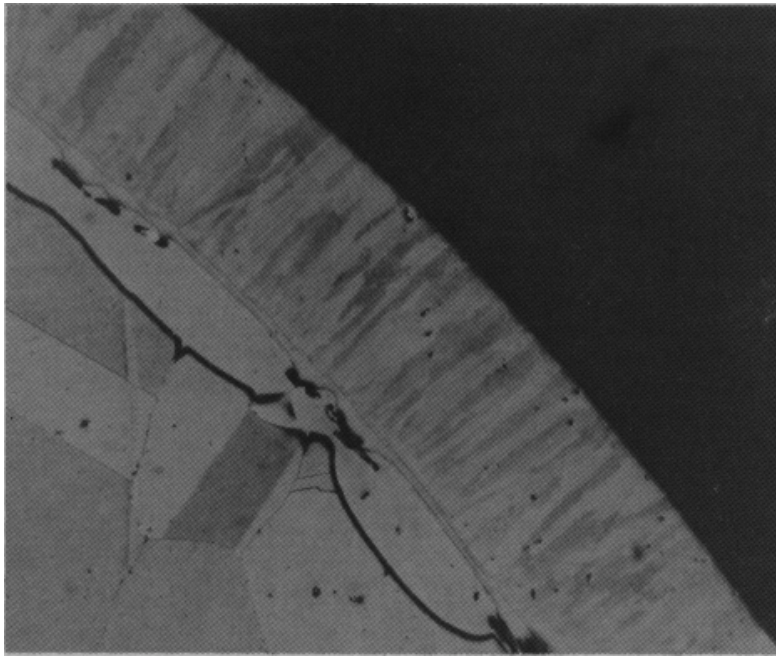


Fig. 7. Computer plot of a properly "framed" 50-point stored curve from orbit 112. The line represents a fit to the electron retardation region and is used in the ground computer analysis to determine T_e . The confidence number is a relative quality indicator of the fit.

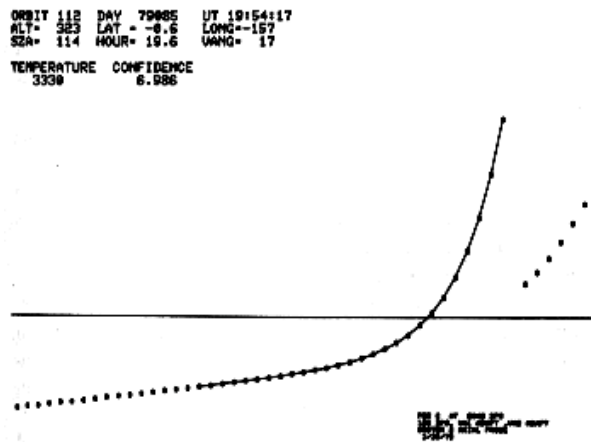


Fig. 8. A computer plot of data from orbit 95. The line segments connect inflight values processed automatically by the instrument. The asterisks are values determined by ground analysis of stored curves. The benefit of using inflight analysis to resolve the fine structure of the ionosphere is apparent.

